OPEN ACCESS Freely available online

PLOS ONE

Multi-Year Lags between Forest Browning and Soil Respiration at High Northern Latitudes

Ben Bond-Lamberty[1]*, Andrew G. Bunn[2], Allison M. Thomson[1]

1 Pacific Northwest National Laboratory, Joint Global Change Research Institute at the University of Maryland–College Park, College Park, Maryland, United States of America, **2** Department of Environmental Sciences, Huxley College, Western Washington University, Bellingham, Washington, United States of America

Abstract

High-latitude northern ecosystems are experiencing rapid climate changes, and represent a large potential climate feedback because of their high soil carbon densities and shifting disturbance regimes. A significant carbon flow from these ecosystems is soil respiration (R_S, the flow of carbon dioxide, generated by plant roots and soil fauna, from the soil surface to atmosphere), and any change in the high-latitude carbon cycle might thus be reflected in R_S observed in the field. This study used two variants of a machine-learning algorithm and least squares regression to examine how remotely-sensed canopy greenness (NDVI), climate, and other variables are coupled to annual R_S based on 105 observations from 64 circumpolar sites in a global database. The addition of NDVI roughly doubled model performance, with the best-performing models explaining ~62% of observed R_S variability. We show that early-summer NDVI from previous years is generally the best single predictor of R_S, and is better than current-year temperature or moisture. This implies significant temporal lags between these variables, with multi-year carbon pools exerting large-scale effects. Areas of decreasing R_S are spatially correlated with browning boreal forests and warmer temperatures, particularly in western North America. We suggest that total circumpolar R_S may have slowed by ~5% over the last decade, depressed by forest stress and mortality, which in turn decrease R_S. Arctic tundra may exhibit a significantly different response, but few data are available with which to test this. Combining large-scale remote observations and small-scale field measurements, as done here, has the potential to allow inferences about the temporal and spatial complexity of the large-scale response of northern ecosystems to changing climate.

Citation: Bond-Lamberty B, Bunn AG, Thomson AM (2012) Multi-Year Lags between Forest Browning and Soil Respiration at High Northern Latitudes. PLoS ONE 7(11): e50441. doi:10.1371/journal.pone.0050441

Editor: Gil Bohrer, The Ohio State University, United States of America

Received August 3, 2012; **Accepted** October 22, 2012; **Published** November 26, 2012

Funding: This research was supported by the US Department of Energy Office of Science, and the authors gratefully acknowledge support from NASA's Land Cover/Land Use Change program (award 08-LCLUC08-1-0043) to AGB. The funders had no role in study design, data collection and analysis, decision to publish, or preparation of the manuscript. This study would not have been possible without the many researchers who collected and published the data used here.

Competing Interests: BBL is a PLOS ONE Editorial Board member. This does not alter the authors' adherence to all the PLOS ONE policies on sharing data and materials.

* E-mail: bondlamberty@pnnl.gov

Introduction

Climate changes in the coming century may affect permafrost thaw rates, greenhouse gas fluxes, wildfires, productivity, biota, and energy fluxes in northern ecosystems [1,2,3,4]. Such high-latitude ecosystems represent a large potential climate feedback [5,6] because of their high soil carbon densities [7] and rapid warming [8]. Any current or future carbon losses from these areas will mostly occur through combustion [9] or changes in the balance between net primary production and the heterotrophic component of R_S, the soil surface CO_2 flux between the soil and atmosphere. At 80–100 Pg C yr^{-1} [10,11], total R_S is one of the largest fluxes in the terrestrial carbon cycle but its magnitude and dynamics remain poorly constrained.

We hypothesized that boreal tree stress or mortality [12,13] might be exerting a significant effect on the large-scale, high-latitude R_S flux, as belowground carbon allocation drops in weakening or dying trees. Such forest stress and mortality has been observed in both boreal North America [14,15] and Eurasia [16,17], as well as more broadly worldwide [18]. These events are most frequently attributed to drought stress [19] or insect attack [20], and can be observed as trends in the remotely-sensed Normalized Differenced Vegetation Index (NDVI), a measure of canopy greenness [21,22], as well as the Enhanced Vegetation Index (EVI) [23]. Such severe stress events are associated with canopy defoliation and depletion of carbon reserves, delayed recovery of surviving individuals, and tree death [24,25]. Because plant photosynthesis is the ultimate source of all ecosystem respiration, and forest soil respiration at large scales may be driven more by productivity than temperature [26], such events should also, in theory, be observable in R_S data.

More generally, climate changes appear to be observable in the extant published record of R_S fluxes [10], but how such large-scale changes interact to affect the major components of the high-latitude carbon cycle remains an open question [6]. To explore one aspect of this, we linked a global R_S database [27], NDVI or canopy greenness [22,28] and gridded climate data using both machine-learning and classical statistical approaches. Our objectives were to analyze the relationship, if any, between forest 'browning' observed from satellites and large-scale patterns of annual R_S, and to infer constraints that may be operating at high latitudes on this large carbon flux.

Methods

Soil Respiration, NDVI, and Ancillary Data

Observed soil surface CO_2 flux, or soil respiration (R_S, g C m^{-2} yr^{-1}), was the primary response variable considered in this study. We used a recent version (20110224a, downloaded 24 February 2011 from http://code.google.com/p/srdb/) of a global soil respiration database [27]. The downloaded data were filtered to include only non-manipulated ecosystems (no agriculture or experimentally manipulated systems); positive R_S values; >50°N latitude; mean annual air temperature (1961–1990) of <2°C, following [10]; and measured using infrared gas analyzers or gas chromatography, relatively standardized techniques.

The primary independent data were Advanced Very High Resolution Radiometer-Normalized Difference Vegetation Index (AVHRR-NDVI, from http://glcf.umiacs.umd.edu/data/gimms/) data covering all land surfaces above 50°N, except the glaciated areas of Greenland. These NDVI measure 'greenness,' which at the pixel level declines (and 'browning' increases) as forests weaken and eventually die from biotic or abiotic stresses. These data were produced as part of the NASA Global Inventory, Monitoring and Modeling project (GIMMS version-G), spanned the years 1982–2008 and were relatively coarse in spatial (64 km^2 cells) and temporal (15-day composite images) scales. GIMMS version-G data have been calibrated to account for orbital drift, cloud cover, sensor degradation, and the emission of volcanic aerosols [29,30]. We transformed these data to a stereographic polar projection based on the Clarke 1866 spheroid, and summarized them at a variety of temporal scales: monthly; seasonal, including spring (mean of March and April), early summer (May, June), late summer (July, August), autumn (September, October), and winter (November-February); and annual (mean of the entire year).

A variety of ancillary data were included in the analysis. Time since disturbance (in years) was derived from the soil respiration database, above, with missing data assigned the median value (~50 years) as recommended by [31]. (Excluding the missing data resulted in a significantly smaller data set, but did not change the disturbance-related results below.) Global climate data ("Monthly Mean Air Temperature (Global 1900–2008)" and "Monthly Total Precipitation (Global 1900–2008)") sets were downloaded from http://climate.geog.udel.edu/~climate/; these data were used because of their spatial resolution and currency. Mean (1961–1990) values and climate anomalies were then computed as the year-specific temperature or precipitation value minus the mean value for that 0.5° grid cell. Global leaf area index (5′, from ECOCLIMAP [32]), grid area (0.5°, to derive a circumpolar flux from area-normalized predictions, from EOS-WEBSTER at http://eos-webster.sr.unh.edu/), nitrogen deposition (5°, from ORNL DAAC at http://webmap.ornl.gov/wcsdown/wcsdown.jsp?dg_id=830_2), a Thornwaite-based climate index [33], and the MODIS Vegetation Continuous Field (Collection 4, Version 3, from http://www.landcover.org/data/vcf/) were also used.

These data sets were matched spatially and temporally to the collected R_S studies using a nearest-neighbor algorithm. Temporally, each R_S observation was paired with climate and NDVI data from the year of that study as well as up to five years previously, i.e., a given R_S observation from year t was associated with temperature anomaly, precipitation anomaly, and NDVI (half-monthly, monthly, etc., as described above) data from year t, t-1, … t-5. This was done because multi-year carbon pools in northern ecosystems [34] may decouple observed carbon fluxes (e.g., tree growth) from ambient abiotic drivers [22,35].

Table 1. Summary of variable importance in conditional inference random forest models.

Variable name	Rank	Models	Variable description
ndvi_jun4	1.4	5	NDVI, June, 4 years previous
ndvi_jun1	2.3	11	NDVI, June, previous year
ndvi_juna1	2.4	5	NDVI, first half of June, previous year
ndvi_maya3	3.7	3	NDVI, first half of May, 3 years previous
ndvi_sepa1	4.6	5	NDVI, first half of September, previous year
ndvi_esummer4	4.7	7	NDVI, early summer, 4 years previous
ndvi_esummer1	5.2	16	NDVI, early summer, previous year
ndvi_jun0	5.3	12	NDVI, June, previous year
ndvi_juna4	5.5	2	NDVI, first half of June, 4 years previous
ndvi_junb4	5.5	2	NDVI, second half of June, 4 years previous
ndvi_juna5	7.0	1	NDVI, first half of June, 5 years previous
ndvi_may3	8.1	7	NDVI, May, 3 years previous
ndvi_apr3	9.0	1	NDVI, April, 3 years previous
ndvi_auga2	9.3	4	NDVI, first half of August, 2 years previous
ndvi_lsummer5	9.3	4	NDVI, late summer, 5 years previous

Only the top 15 variables (out of 270 total potential predictors) are shown. Variables are ordered by the mean rank (from node purity) computed by the random forest algorithm; the third column gives number of models across which this mean was computed.

doi:10.1371/journal.pone.0050441.t001

Data Analysis

Two related machine-learning algorithms were used on the final, unified data set (105 observations and 288 variables, from 64 unique sites). The standard Random Forest algorithm [31], a nonparametric machine learning technique for classification and regression, is widely used for large-data analyses, and as a data-driven methodology makes no *a priori* theoretical assumptions about R_S drivers or behavior. The algorithm predicts by aggregating regression trees constructed using different random samples of the data, and choosing splits of the trees from subsets of the available predictors, which are randomly chosen at each node [31]. The use of random data and predictor subsets means that the full data set can be used and data need not be withheld for validation. The RF algorithm generally produces highly accurate and unbiased estimates and classification when potential predictors are drawn from the same scale or category, and it is particularly robust against overprediction for 'm>n' (more potential predictor variables than observations) data sets.

Random Forest can be unreliable (exhibit biased variable selection), however, when potential predictor variables vary in measurement scale or categories [36]. For this reason we also used a conditional inference random forest (CI-RF) algorithm [37], the *cforest* routine in *party* package version 0.9-99991 in R [38]. This algorithm supports conditional inference trees [37] and aggregates using observation weights extracted from the trees [39]. Such conditional inference forests better handle variables of different types, and observations of different weights, than do trees generated using the original Breiman RF algorithm, although they do not entirely eliminate the preference for correlated predictors [37].

We allowed these algorithms to access varying amounts of NDVI (from the original 15-day data, to monthly, seasonal, and annual means, to none at all) and previous-year information ('lookback,' from 0 to 5 years in the past). Importantly, each level

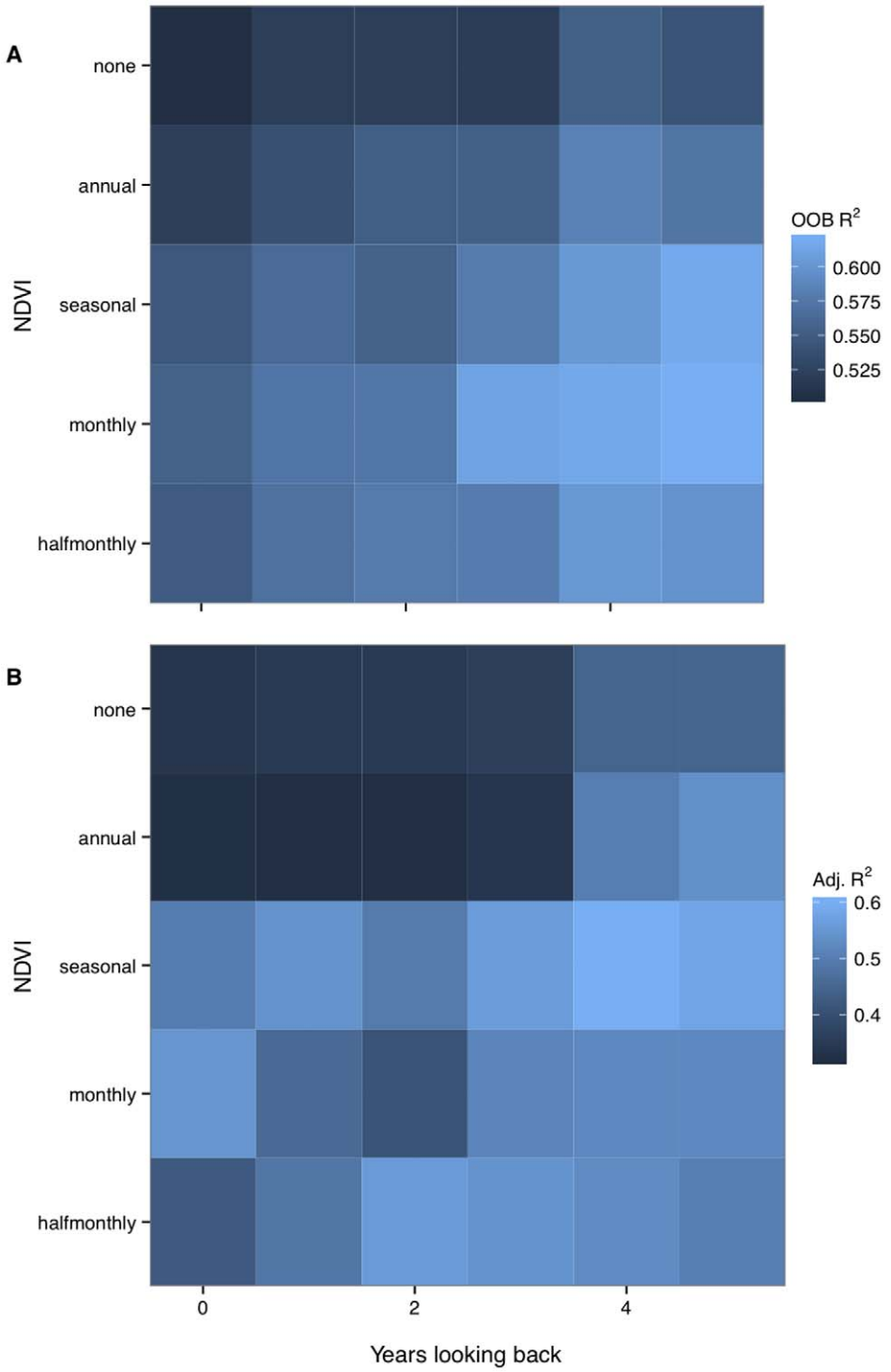

Figure 1. Summary of model performance in predicting high-latitude soil respiration. Data are shown by algorithm type (a: conditional inference Random Forest, CI-RF; b: ordinary least squares, OLS), level of NDVI detail available to the algorithm (none, and annual, seasonal, monthly, and half-monthly means), and number of years the algorithm was allowed to look into the past. Values given are bin midpoints; out-of-bag R^2 for CI-RF (see Methods), and adjusted R^2 for OLS.
doi:10.1371/journal.pone.0050441.g001

tested included all previous coarser ones; for example, models using monthly NDVI data were also given seasonal and annual data, to see if the new level of detail resulted in significant model improvement. Because late-winter snow interferes with the satellite sensor, resulting in many missing values for this time period, we excluded December-April NDVI after extensive testing: none of these data was significant (i.e., ranked in the top 25 most important variables; cf. **Table 1**) in any tested R_S model, and their exclusion resulted in no decrease in model explanatory power. The RF and CI-RF routines were run with default settings (in particular,

Table 2. Summary of the best-performing ordinary least squares (OLS) model.

Variable	Year	Estimate	SE	t	P	Signif.
(Intercept)		−16760	9687	−1.73	0.087	.
NDVI (early summer)	1	13.96	5.02	2.78	0.007	**
NDVI (late summer)	4	7.77	5.15	1.51	0.135	
NDVI (early summer)	0	6.85	4.81	1.43	0.158	
Air temperature	4	1.03	1.66	6.21	<0.001	***
NDVI (late summer)	1	−1.53	4.96	−3.08	0.003	**
Precipitation	0	0.70	0.34	2.05	0.043	*
Year		8.51	4.84	1.76	0.082	.
Air temperature	0	−55.19	22.81	−2.42	0.017	*
Mean annual precip.		−0.58	0.20	−2.90	0.005	**
NDVI (annual)	1	−14.43	6.31	−2.29	0.025	*
NDVI (fall)	0	9.21	3.35	2.75	0.007	**

Potential parameters of the best OLS model (RMSE = 156.9 g C m^{-2} yr^{-1} on 94 d.f., adjusted $R^2 = 0.61$, $P<0.001$) were selected by the CI-RF algorithm before OLS was performed (see Methods and Table 1). Columns include variable included in OLS regression, year of data stream (0 = current year, 1 = previous year, etc.); OLS estimate and standard error (SE); t-value; P-value; and significance ("." <0.1; "*" <0.05; "**" <0.01; "***" <0.001).
doi:10.1371/journal.pone.0050441.t002

number of variables randomly selected at each node = 5, number of trees = 500) for all 30 models (5 levels of NDVI information times 6 levels of temporal lookback); we found that altering these parameters did not change the results in any meaningful way. The algorithms ranked all variables by importance. For CI-RF, we computed a pseudo-R^2 following the original *randomForest* package, as 1-SS_{TOT}/SS_{ERR}, because the *party* package does not currently compute a true out-of-bag error rate.

We also examined the effect of including the most important variables, as identified by the RF and CI-RF algorithms, into ordinary least squares (OLS) models, as OLS is a fundamental tool for analyzing sources of variance in many studies. For each of the 30 NDVI/lookback models we built ordinary least squares (OLS) models using the 18 most important variables identified by the machine-learning algorithms. The automated 'step' function in R removed and added model terms, starting from the complete formula identified by the RF (and CI-RF) analysis. Term selection was based on Akaike Information Criterion. For all analyses, observations were weighted by the years of observed data reported for each R_S data point, to account for studies that reported multi-year R_S means. OLS models were checked for influential outliers using a Cook's distance threshold of 0.5 and refit, if necessary, after outlier removal.

Circumpolar Modeling

The best-performing (based on pseudo-R^2) model was used to predict R_S fluxes across the circumpolar region. A circumpolar 0.5° grid was used, with grid cells matched to all required climate, NDVI, and ancillary data. Predicted fluxes for years 1989–2008–roughly the period of methodologically standardized and published R_S measurements [10]–were calculated using the cell area data and summed to produce a global high-latitude flux for boreal and Arctic (>50°N, mean annual air temperature <2°C) cells. A nonparametric Mann-Kendall test was used to test for temporal trends in the model output, and D'Agostino's K^2 goodness-of-fit [40] to test for skew or departures from normality. All analyses were performed using R 2.15.1 [38].

Results

The two machine-learning models accounted for 50–62% of the observed variability for 105 annual R_S observations at high latitudes. When allowed to use more-detailed NDVI data, and look back further into the past (i.e., consider previous-year conditions to explain current R_S) the models' performance improved (**Figure 1**). The best-performing model (a CI-RF type, root mean square error RMSE = 139.9 g C m^{-2} yr^{-1}) used monthly NDVI and up to five previous years' NDVI/climate data; this was also identified as the best model by the classical RF algorithm. OLS models built using the most important variables from the machine-learning analyses showed a dramatic improvement, with explained variability almost doubling from 33% (no NDVI, only current-year data) to 61% (seasonal NDVI, up to four years 'lookback' allowed). The best-performing OLS model is summarized in **Table 2**. For all algorithms, the use of half-monthly NDVI did not improve model performance relative to mean monthly NDVI.

Previous-year NDVI–in particular, early-summer greenness–was generally the most important R_S predictor. Nine of the top ten CI-RF variables, and five of the top ten RF ones, were NDVI in early summer (May, June, July) in years before the R_S measurement, especially the previous year (Table 1). The best-performing models also followed this pattern, with previous-year June NDVI the best predictor and previous-year temperature the best non-NDVI predictor. A number of potential explanatory variables were almost never highly ranked, including nitrogen deposition, time since disturbance, leaf area index, and percent tree cover. As in a previous study [10], mean annual air temperature was negatively associated with R_S–i.e., warmer years were consistently associated with lower respiration at high latitudes. In summary, NDVI proved a far better R_S predictor than any other type of variable; previous-year data almost always outperformed current-year data; and early-summer NDVI was the single best predictor across a large number of models.

The results of extrapolating R_S across the circumpolar boreal region based on NDVI and climate data for the 1989–2008 period are shown spatially in **Figure 2**, and the integrated circumpolar flux in **Figure 3**. Predicted R_S values ranged from 212–646 g C m^{-2} yr^{-1}, with a mean±s.d. of 348±102 g C m^{-2} yr^{-1}; in comparison, Arctic and boreal data average 109±109 and 383±228 g C m^{-2} yr^{-1}, respectively, in the R_S database used here [27].

The model did not predict extremely low (<100 g C m^{-2} yr^{-1}) R_S values observed at some Arctic sites, probably due both to the paucity of observed R_S data at these extreme latitudes, and the presence of late-lying snow that interferes with the satellite sensor. High observed R_S values also tended to be underpredicted (**Figure 4**). The mean predicted R_S integrated over the entire study area was 8.6 Pg C yr^{-1}, ~9% of the global flux [10], and declined (0.04 Pg yr^{-2}, Mann-Kendall tau = -0.511, $P = 0.049$) over the last ten years of the study period. Large areas of declining R_S in western North America (yellow patches in **Figure 2**) drove the circumpolar slowdown in the model output.

Discussion

The dominance of lag effects–in previous-year NDVI and air temperature–in this analysis is consistent with both theory and observations. Short-turnaround, labile C comprises a significant component of ecosystem C fluxes [41], while field experiments

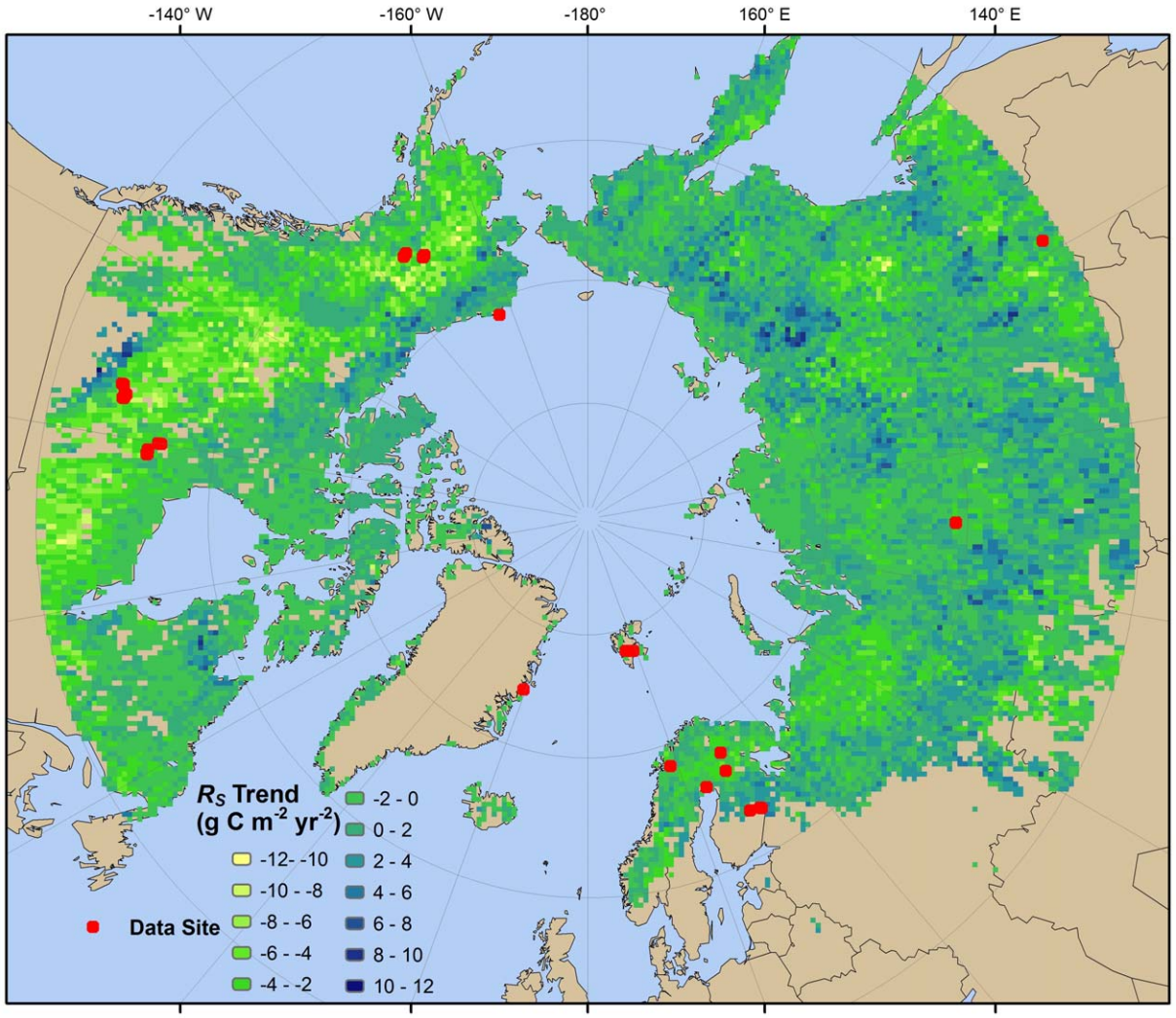

Figure 2. Spatial distribution of 1989–2008 soil respiration trends (R_S, g C m^{-2} yr^{-2}). Grid cells are colored by slope of R_S trend, computed based on the best fitting model (conditional-inference Random Forest, using monthly NDVI data up to 5 years previously) from Table 1. Field studies used in building the models, drawn from a global R_S database [27], are shown by overlaid points.
doi:10.1371/journal.pone.0050441.g002

have shown a lack of correlation between boreal tree ring width increment and net ecosystem exchange [35], while ring width and NDVI are only inconsistently correlated in high-latitude forests [42,43]. This suggests that multi-year C pools play a significant role in buffering ecosystem carbon fluxes from changing abiotic drivers. Lags between R_S and its drivers (soil temperature and gross primary production) of up to 88 days were shown by Vargas et al. [44], but we are unaware of previous studies documenting multi-year lag effects. We note that RF and CI-RF models using no current-year data at all–simply previous-year NDVI, air temperature, and precipitation–explains ~60% (RMSE = 140.9 g C m^{-2} yr^{-1}) of observed R_S variability, i.e., adding current-year data yields very little improvement in model performance.

What mechanisms would link increases in temperature with declines in R_S, as observed here? Largely following the logic of Peng et al. [14], we hypothesize that drought and water stress engender hydraulic failure and inability to maintain carbon balance (i.e., starvation) [25]. The dominant sources of R_S are root (autotrophic) and microbial (heterotrophic) respiration, and both are affected–albeit at different temporal lags–by changes in the photosynthate supply [45]. The resulting declines in belowground tree respiration and root exudates then depress the R_S flux as measured at the soil surface.

Such a mechanism would be consistent with other studies performed at a variety of scales. Drought has deleterious effects on CO_2 uptake [46], and has been shown to reduce R_S in field studies [47]. Tree mortality in western boreal North America has increased [14], and field studies have observed aspen and white spruce stress and dieback in North America has been linked to moisture indices [12]. Silva et al. [15] reported that temperate and boreal trees in Ontario, Canada, exhibited widespread growth decline consistent with warming-induced stress, in spite of increases in water use efficiency over the last half-century. At larger scales, FLUXNET analyses have inferred significant drought effects on ecosystem carbon cycling [48,49], and productivity (for which NDVI, in this study, is a proxy) has been shown to be more important than temperature in determining landscale-level R_S [26]. Finally, remote sensing analyses suggest that changes in annual temperature and precipitation across North America are negatively affecting forest resilience as measured

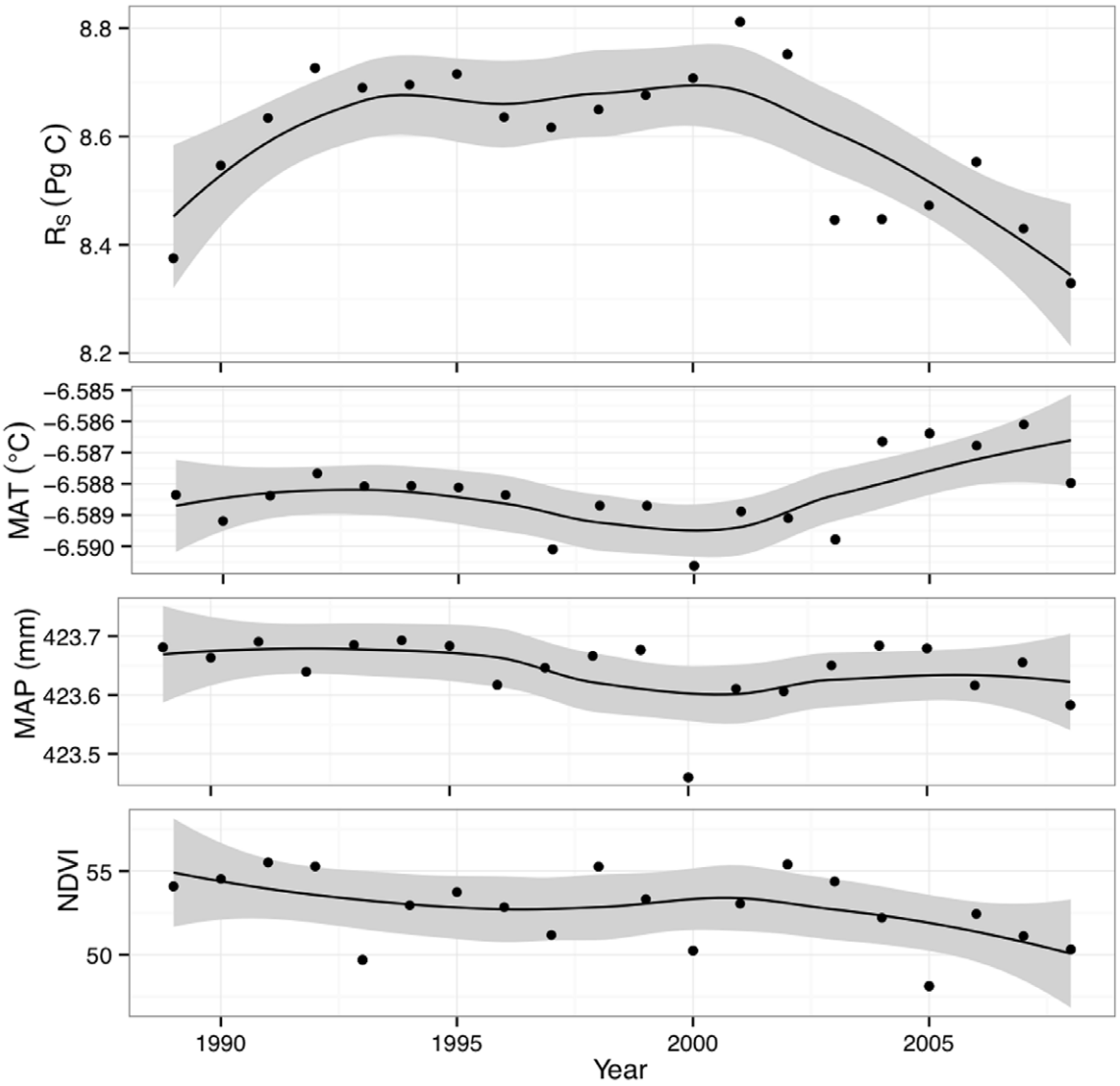

Figure 3. Predicted high-latitude soil respiration (R_S), by year, with main driver variables. Panels show, from top, R_S predicted flux; mean annual temperature (MAT); mean annual precipitation (MAP); and previous-June canopy greenness (NDVI, unitless). R_S points show integrated result of the best-performing Random Forest model; to highlight trend, a loess smoother is shown by the dark line. Smoother errors (gray regions) were computed as the least-squares error on locally weighted scatterplot smoothing.
doi:10.1371/journal.pone.0050441.g003

using the MODIS Enhanced Vegetation Index [23]. The use of previous-year NDVI in this study is thus a significant strength, as it provides an integrated signal of forest canopy stress tightly linked with the photosynthates stored for the following year's growth and respiration.

There are other possible mechanisms to explain a putative R_S slowdown: climate changes might enable more pathogen and pest outbreaks in drought-weakened trees [25] or increase freeze-thaw events [12], for example, resulting in tree death, lower NDVI and lower R_S. Increased nitrogen deposition could also be depressing forest R_S, as has been shown to occur in temperate forests [50], although most North American boreal and Arctic sites are considered nitrogen-limited. We found no association between R_S and nitrogen deposition and thus a water-related mechanism, as laid out above, seems more consistent with the available data.

It is not surprising that time since disturbance exerted no effect on R_S in this analysis. This is not to say that disturbance exerts no effect: plant productivity exerts a dominant role on R_S [26], and fire in particular plays an important role in many high-latitude forests [51], altering R_S by killing plants, increasing litter inputs, changing soil moisture conditions, and increasing the active layer depth [52]. Disturbances can also cause soil C losses (via R_S) so large that sites become multi-year carbon sources [26]. The time-since-disturbance variable may simply not have added any extra information, however, given the strong NDVI effect found in this analysis and the fact that NDVI and time since disturbance tend to be well-correlated for several decades following disturbance [53]. In addition, while post-disturbance R_S changes may be visible in meta-analyses [54] and syntheses [26], many studies have observed inconsistent or invariant ecosystem respiration [55] and R_S [56] in the decades after disturbance. Finally, relatively few R_S studies have been performed in post-disturbance forest and tundra [27].

This analysis has a number of limitations. First, although we used two more years of data (observations published 2009–2010) than a previous R_S meta-analysis [10], these results are based on

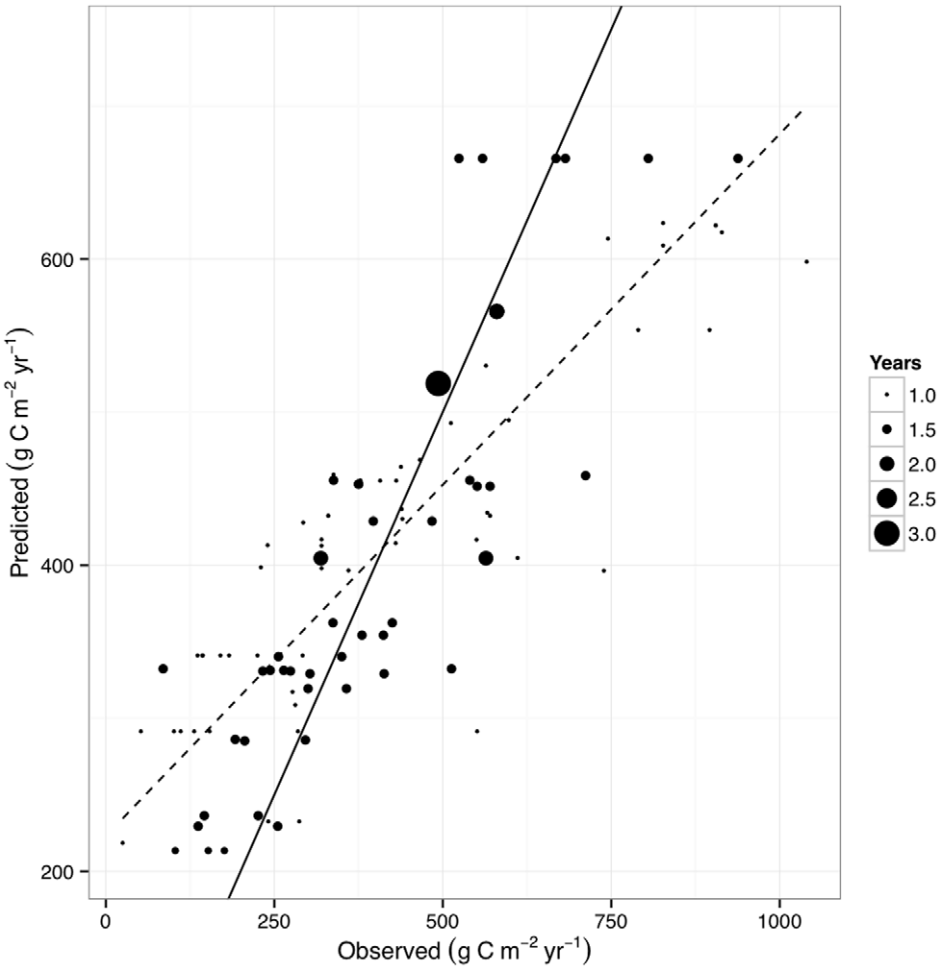

Figure 4. Observed versus predicted soil respiration (g C m^{-2} yr^{-1}) for the best-performing linear model summarized in Table 1. Solid line shows 1:1, dashed line (with grey error region) the relationship between observed and predicted values. Point size indicates number of years reported by each study (cf. Figure 2), and was used as a weighting factor in all analyses.
doi:10.1371/journal.pone.0050441.g004

only 105 annual flux measurements spread across a large ($\sim 24\times10^6$ km^2) circumpolar region. The possibility of a type I (false positive) error remains [10] significant: future data may resolve the curiosity of high-latitude R_S changes not being positively correlated with air temperature increases. Second, the R_S data used here are dominated by well-drained, boreal, upland sites, reflecting an imbalance in the published literature [27]. But the respiration of peatland and permafrost ecosystems–which store an outsized fraction of global soil organic carbon–may change in different ways than a simple temperature- and NDVI-based model would predict, driven by species shifts, permafrost thaw, and increasing peat oxygenation. Tundra ecosystems will also likely respond differently to warming than will boreal forests, as processes such as warming-induced thermokarst and woody plant encroachment may increase plant productivity [6,57,58]. Finally, R_S cannot by itself be used to infer carbon balance, as ecosystem carbon balance is driven by the balance between net primary production and heterotrophic respiration from snags, woody debris, and soil. Few such comprehensive data are available at high latitudes, however.

Conclusions

This study has shown that remotely-sensed NDVI and climate data explain a large fraction of the variability of R_S, the dominant component of ecosystem respiration, at high latitudes. Combining large-scale observations (NDVI) and a compilation of small-scale observations (R_S) allowed us to show that lag effects imply multi-year carbon pools exerting significant large-scale effects, to the point that no current-year data are needed (at this scale) to predict total R_S in a given year. Finally, we suggest that high-latitude R_S has declined significantly over the last ten years, as warmer summers stress some northern ecosystems, in particular the boreal forests that constitute most of the data used here [46]; we caution that tundra ecosystems may respond very differently. Although we cannot prove causality between the observed NDVI and R_S data, such an effect would be consistent with other recent studies (e.g., [59]). Because the boreal and Arctic carbon cycles may exert strong global climate feedbacks [6], the question of whether this decline is truly a symptom of water stress and forest mortality deserves further exploration.

Author Contributions

Conceived and designed the experiments: BBL AGB AMT. Performed the experiments: BBL AGB. Analyzed the data: BBL AGB AMT. Contributed reagents/materials/analysis tools: BBL AGB AMT. Wrote the paper: BBL AGB AMT.

References

1. Field CB, Lobell DB, Peters HA, Chiariello NR (2007) Feedbacks of terrestrial ecosystems to climate change. Annual Review of Environment and Resources 32: 1–29.
2. Schaefer K, Zhang T, Bruhwiler LP, Barrett AP (2011) Amount and timing of permafrost carbon release in response to climate warming. Tellus Series B-Chemical and Physical Meteorology 63: 165–180.
3. Johnstone JF, McIntire EJB, Pedersen EJ, King G, Pisaric MJF (2010) A sensitive slope: estimating landscape patterns of forest resilience in a changing climate. Ecosphere 1.
4. Beck PSA, Juday GP, Alix C, Barber VA, Winslow SE, et al. (2011) Changes in forest productivity across Alaska consistent with biome shift. Ecology Letters 14: 373–379.
5. Schuur EAG, Vogel JG, Crummer KG, Lee H, Sickman JO, et al. (2009) The effect of permafrost thaw on old carbon release and net carbon exchange from tundra. Nature 459: 556–559.
6. McGuire AD, Anderson LG, Christensen TR, Dallimore S, Guo L, et al. (2009) Sensitivity of the carbon cycle in the Arctic to climate change. Ecological Monographs 79: 523–555.
7. Tarnocai C, Canadell JG, Schuur EAG, Kuhry P, Mazhitova G, et al. (2009) Soil organic carbon pools in the northern circumpolar permafrost region. Global Biochemical Cycles 23: GB2023.
8. IPCC (2007) Summary for Policymakers. In: Solomon SD, Qin D, Manning MR, Chen Z, Marquis M et al., editors. Climate Change 2007: The Physical Science Basis Contribution of Working Group I to the Fourth Assessment Report of the Intergovernmental Panel on Climate Change. Cambridge, UK and New York, NY, USA: Cambridge University Press. 18.
9. Turetsky MR, Kane ES, Harden JW, Ottmar RD, Manies KL, et al. (2011) Recent acceleration of biomass burning and carbon losses in Alaskan forests and peatlands. Nature Geoscience 4: 27–31.
10. Bond-Lamberty B, Thomson AM (2010) Temperature-associated increases in the global soil respiration record. Nature 464: 579–582.
11. Raich JW, Potter CS, Bhagawati D (2002) Interannual variability in global soil respiration, 1980–94. Global Change Biology 8: 800–812.
12. Hogg EH, Brandt JP, Kochtubajda B (2005) Factors affecting interannual variation in growth of western Canadian aspen forests during 1951–2000. Canadian Journal of Forest Research 35: 610–622.
13. Frey BR, Lieffers VJ, Hogg EH, Landhäusser SM (2004) Predicting landscape patterns of aspen dieback: mechanisms and knowledge gaps. Canadian Journal of Forest Research 34: 1379–1390.
14. Peng C, Ma Z, Lei X, Zhu Q, Chen H, et al. (2011) A drought-induced pervasive increase in tree mortality across Canada's boreal forests. Nature Climate Change 1: 467–471.
15. Silva LCR, Anand M, Leithead MD (2010) Recent widespread tree growth decline despite increasing atmospheric CO_2. PLoS ONE 5: e11543.
16. Dulamsuren C, Hauck M, Leuschner C (2010) Recent drought stress leads to growth reductions in Larix sibirica in the western Khentey, Mongolia. Global Change Biology 16: 3024–3035.
17. Wu X, Liu H, Guo D, Anenkhonov OA, Badmaeva NK, et al. (2012) Growth decline linked to warming-induced water limitation in hemi-boreal forests. PLoS ONE in press.
18. Allen CD, Macalady AK, Chenchouni H, Bachelet D, McDowell NG, et al. (2010) A global overview of drought and heat-induced tree mortality reveals emerging climate change risks for forests. Forest Ecology and Management 259: 660–684.
19. van Mantgem PJ, Stephenson NL, Byrne JC, Daniels LD, Franklin JF, et al. (2009) Widespread increase of tree mortality rates in the western United States. Science 323: 521–524.
20. Goetz SJ, Bond-Lamberty B, Harmon ME, Hicke JA, Houghton RA, et al. (2012) Observations and assessment of forest carbon recovery following disturbance in North America. Journal of Geophysical Research-Biogeosciences 117: G02022.
21. Beck PSA, Goetz SJ (2011) Satellite observations of high northern latitude vegetation productivity changes between 1982 and 2008: ecological variability and regional differences. Environmental Research Letters 6: 045501.
22. Bunn AG, Goetz SJ (2006) Trends in satellite-observed circumpolar photosynthetic activity from 1982 to 2003: the influence of seasonality, cover type, and vegetation density. Earth Interactions 10: 1–19.
23. Li S, Potter CS (2012) Vegetation regrowth trends in post forest fire ecosystems across North America from 2000 to 2010. Natural Science in press.
24. Galiano L, Martínez-Vilalta J, Lloret F (2011) Carbon reserves and canopy defoliation determine the recovery of Scots pine 4 yr after a drought episode. New Phytologist.
25. McDowell NG (2011) The interdependence of mechanisms climate-driven vegetation mortality. Trends in Ecology and Evolution 26: 523–532.
26. Janssens IA, Lankreijer H, Matteucci G, Kowalski AS, Buchmann N, et al. (2001) Productivity overshadows temperature in determining soil and ecosystem respiration across European forests. Global Change Biology 7: 269–278.
27. Bond-Lamberty B, Thomson AM (2010) A global database of soil respiration data. Biogeosciences 7: 1915–1926.
28. Goetz SJ, Bunn AG, Fiske GJ, Houghton RA (2005) Satellite-observed photosynthetic trends across boreal North America associated with climate and fire disturbance. Proceedings of the National Academy of Science 102: 13521–13525.
29. Tucker CJ, Pinzon JE, Brown ME, Slayback DA, Pak E, et al. (2005) An extended AVHRR 8-km NDVI dataset compatible with MODIS and SPOT vegetation NDVI data. International Journal of Remote Sensing 26: 4485–4498.
30. Brown ME, Pinzon JE, Tucker CJ (2004) New vegetation index data set to monitor global change. EOS Transactions American Geophysical Union 85: 565.
31. Breiman L (2001) Random forests. Machine Learning 45: 5–32.
32. Masson V, Champeaux JL, Chauvin F, Meriguet C, Lacaze R (2003) A global database of land surface parameters at 1-km resolution in meteorological and climate models. Journal of Climate 16: 1261–1282.
33. Willmott CJ, Feddema JJ (1992) A more rational climate index. The Professional Geographer 44: 84–88.
34. Carbone MS, Czimczik CI, McDuffee KE, Trumbore SE (2007) Allocation and residence time of photosynthetic products in a boreal forest using a low-level 14C pulse-chase labeling technique. Global Change Biology 13: 466–477.
35. Rocha AV, Goulden ML, Dunn AL, Wofsy SC (2006) On linking interannual tree ring variability with observations of whole-forest CO_2 flux. Global Change Biology 12: 1378–1389.
36. Strobl C, Boulesteix A-L, Zeileis A, Hothorn T (2007) Bias in random forest variable importance measures: Illustrations, sources and a solution. BMC Bioinformatics 8: 25.
37. Strobl C, Boulesteix A-L, Kneib T, Augustin T, Zeileis A (2008) Conditional variable importance for random forests. BMC Bioinformatics 9: 307.
38. R Development Core Team (2012) R: A language and environment for statistical computing. R Foundation for Statistical Computing, Vienna, Austria.
39. Hothorn T, Buehlmann P, Dudoit S, Molinaro A, Van Der Laan M (2006) Survival ensembles. Biostatistics 7: 355–373.
40. D'Agostino RB (1970) Transformation to normality of the null distribution of g_1. Biometrika 57: 679–681.
41. Knorr W, Prentice IC, House JI, Holland EA (2005) Long-term sensitivity of soil carbon turnover to warming. Nature 433: 298–301.
42. Bunn AG, Goetz SJ, Fiske GJ (2005) Observed and predicted responses of plant growth to climate across Canada. Geophysical Research Letters 32: L16710 (16714 pp.).
43. Berner LT, Beck PSA, Bunn AG, Lloyd AH, Goetz SJ (2011) High-latitude tree growth and satellite vegetation indices: Correlations and trends in Russia and Canada (1982–2008). Journal of Geophysical Research-Biogeosciences 116: G01015.
44. Vargas R, Baldocchi DD, Allen MF, Bahn M, Black TA, et al. (2010) Looking deeper into the soil: biophysical controls and seasonal lags of soil CO2 production and efflux across multiple vegetation types. Ecological Applications.
45. Vargas R, Baldocchi DD, Bahn M, Hanson PJ, Hosman KP, et al. (2011) On the multi-temporal correlation between photosynthesis and soil CO2 efflux: reconciling lags and observations. New Phytologist in press.
46. Angert A, Biraud S, Bonfils C, Henning CC, Buermann W, et al. (2005) Drier summers cancel out the CO2 uptake enhancement induced by warmer springs. Proceedings of the National Academy of Science 102: 10823–10827.
47. Burton AJ, Pregitzer KS, Zogg GP, Zak DR (1998) Drought reduces root respiration in sugar maple forests. Ecological Applications 8: 771–778.
48. Schwalm CR, Williams CA, Schaefer K, Arneth A, Bonal D, et al. (2010) Assimilation exceeds respiration sensitivity to drought: A FLUXNET synthesis. Global Change Biology 16: 657–670.
49. Beer C, Reichstein M, Tomelleri E, Ciais P, Jung M, et al. (2010) Terrestrial gross carbon dioxide uptake: global distribution and covariation with climate. Science 329: 834–838.
50. Janssens IA, Dieleman WIJ, Luyssaert S, Subke J-A, Reichstein M, et al. (2010) Reduction of forest soil respiration in response to nitrogen deposition. Nature Geoscience 3: 315–322.
51. Kasischke ES, Turetsky MR (2006) Recent changes in the fire regime across the North American boreal region–Spatial and temporal patterns of burning across Canada and Alaska. Geophysical Research Letters 33: L09703.
52. O'Neill KP, Kasischke ES, Richter DD (2002) Environmental controls on soil CO_2 flux following fire in black spruce, white spruce, and aspen stands of interior Alaska. Canadian Journal of Forest Research 32: 1525–1541.
53. Goulden ML, Winston GC, McMillan A, Litvak M, Read EL, et al. (2006) An eddy covariance mesonet to measure the effect of forest age on land–atmosphere exchange. Global Change Biology 12: 1–17.
54. Pregitzer KS, Euskirchen ES (2004) Carbon cycling and storage in world forests: biome patterns relating to forest age. Global Change Biology 10: 2052–2077.
55. Amiro BD, Barr AG, Barr JG, Black TA, Bracho R, et al. (2010) Ecosystem carbon dioxide fluxes after disturbance in forests of North America. Journal of Geophysical Research-Biogeosciences 115: G00K02.
56. Wang C, Bond-Lamberty B, Gower ST (2002) Soil surface CO_2 flux in a boreal black spruce fire chronosequence. Journal of Geophysical Research-Atmospheres 108: art. no. 8224.
57. Rustad LE, Campbell JL, Marion GM, Norby RJ, Mitchell MJ, et al. (2001) A meta-analysis of the response of soil respiration, net nitrogen mineralization, and

aboveground plant growth to experimental ecosystem warming. Oecologia 126: 543–562.
58. Doak DF, Morris WF (2010) Demographic compensation and tipping points in climate-induced range shifts. Nature 467: 959–962.
59. Piao S, Wang X, Ciais P, Zhu B, Wang T, et al. (2011) Changes in satellite-derived vegetation growth trend in temperate and boreal Eurasia from 1982 to 2006. Global Change Biology 17: 3228–3239.